Advances in Engineering Software 129 (2019) 69–80

Contents lists available at ScienceDirect

Advances in Engineering Software

journal homepage: www.elsevier.com/locate/advengsoft

Auxetic structure design using compliant mechanisms: A topology optimization approach with polygonal finite elements

Cícero R. de Lima[a,*], Glaucio H. Paulino[b]

[a] School of Engineering, Modeling and Applied Social Sciences, UFABC - Federal University of ABC, Rua Arcturus, 03, São Bernardo do Campo, SP 09606-070, Brazil
[b] School of Civil and Environmental Engineering, GeorgiaTech - Georgia Institute of Technology, 790 Atlantic Drive NW, Atlanta, GA 30332-0355, USA

ARTICLE INFO

Keywords:
Topology optimization
Compliant mechanism
Polygonal elements
Auxetic material
Additive manufacturing

ABSTRACT

Compliant mechanisms are monolithic structures where the movement is given by the flexibility of the structure rather than the presence of joints and pins. The absence of joints allows the construction of compliant mechanisms in microscale. In this work, the compliant mechanism is designed by using topology optimization to generate microstructure unit cells that simulate the effect of auxetic materials, i.e. those with negative Poisson's ratio. Polygonal finite element meshes are introduced in the topology optimization formulation to avoid the hinges (one-node connections) in the compliant mechanism design. A pattern repetition constraint is applied to generate auxetic macrostructures. An integrated approach that combines a projection technique with a mapping technique is adopted to include the minimum member size constraint, making the topology optimization results possible to be manufactured. The connection of the topology optimization approach with additive manufacturing is demonstrated using 3D printers based on FFF (fused filament fabrication) and PolyJet technologies. Thus, computational simulation in connection with rapid prototyping are carried out to verify the results.

1. Introduction

Compliant mechanisms are mechanisms whose motion is given by its flexible structural body rather than the presence of joint and pins (articulation members) [1]. Unlike conventional mechanisms, which are structures composed of rigid bodies connected by joints, a compliant mechanism is a monolithic structure that explores the deformation property as source of motion.

Compliant mechanisms have wide application in devices that involve precision mechanics, such as mechanisms of cameras, reader head of a computer hard drive, piezoelectric transducers, among others known as Micro-Electro-Mechanical Systems (MEMS) [2], in which due to the compact assembly of that devices, small parts and smaller number of components are required, otherwise the slack problem in the assembling can make operation of the device impracticable.

The motion presented in the most of MEMS devices can be accomplished with small displacements generated by compliant mechanisms. Nevertheless, compliant mechanism can also be used in the design of grippers, jaws or scissors that requires precise motion, such as medical surgical instruments. In fact, compliant mechanisms have potential application in many branches of engineering (biomedical, aerospace, automation and robotics, among others).

1.1. Design of compliant mechanism

However, the generic design of a compliant mechanism is a very complex task, since essentially ones want to know the following: what is the best topology and shape to the structure, which generates motion in a desired direction to a given region of the structure, considering a certain force applied in another point and direction? The structural optimization is a theoretical approach adopted in this paper to address that question to the compliant mechanism design, whose focus is to obtain the flexibility distributed in the structure of the mechanism.

A very promising method for this purpose is the topology optimization method (TOM). Essentially, the method seeks the optimized distribution of material within a fixed design domain (initial region that will limit the space occupied by the mechanisms), by removing and adding material in each point of that domain in order to minimize (or maximize) a specified objective function, satisfying given constraints imposed in the optimization problem. Unlike other methods, such as the shape optimization and parametric optimization [3], the TOM requires no prior knowledge of the topology of the structure, which is obtained systematically from any initial material distribution, and determines the presence of new holes in the structure, allowing to obtain high mass decrease and a large performance increase [4].

There are several studies that demonstrate the efficiency of the TOM

* Corresponding author.
E-mail addresses: cicero.lima@ufabc.edu.br (C.R. de Lima), paulino@gatech.edu (G.H. Paulino).

https://doi.org/10.1016/j.advengsoft.2018.12.002
Received 25 May 2018; Received in revised form 20 November 2018; Accepted 18 December 2018
Available online 27 December 2018
0965-9978/

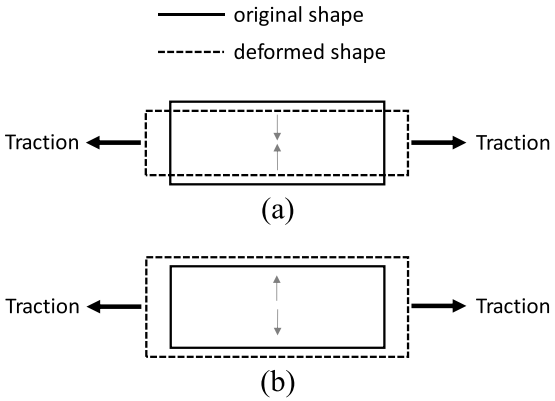

Fig. 1. Behavior of (a) conventional and (b) auxetic materials.

as a tool for design of compliant mechanisms. Among the classic applications presented in the literature, we have the gripper mechanisms [5], the force inverters [6], complex mechanisms with multiple inputs and outputs [7], micromechanics with thermal actuation [8], large-displacement mechanisms [9], and others.

1.2. Application to auxetic structure design

This work focuses on using the TOM to the compliant mechanism design and applied to create a microstructure that simulates the behavior of auxetic materials, that is, an unconventional property material that when tractioned it increases its size in the perpendicular direction to the traction load, and vice-versa when compressed (Fig. 1b).

Unlike conventional materials, an auxetic material has negative Poisson's ratio. The auxetic behavior can provide to structural materials many benefits, since they may acquire notable properties. When compared to conventional materials, it is noticed an improvement of their mechanical properties, such as increased resistance to shear and fracture and better energy absorption capacity [10]. Other notable property of these materials is their greater resistance to impact. Evans and Alderson [11] demonstrate that when the auxetic material is hit by an object, the material flows to the region of impact to reinforce that region, instead of escape way from the impact zone as observed in the conventional materials.

Consequently, these properties make auxetic materials very suitable for various engineering applications, such as smart bandages and filters which adjusting effectively the size of its pores, according to the need [10]. Textile fibers made auxetic material are potentially attractive for applications in protective clothing and accessories for military security, such as bullet-proof vests [11]. A promising engineering field for application of auxetic materials is the Aerospace. Since the auxetic material have better energy absorption and high impact resistance properties, it can potentially be applied to build components of aerospace structures, such as the aircraft nose, for example.

The obtaining of an auxetic material (or auxetic microstructure) is an activity not fully mastered yet, since its design techniques is new and manufacturing is available only under small scale. Some available techniques aim at obtaining auxetic materials through structural transformation of conventional materials, such as foams or polymers. Further details on these techniques can be found in Chan and Evans [12] and Alderson et al. [13].

Another exploited way to obtain an auxetic material is to design a unit cell (microstructure) with auxetic behavior and apply a periodic repetition of this cell over a domain defined to create the macrostructure (auxetic material). Fig. 2 illustrates an auxetic structure obtained through this process, using a reentrant periodic cell structure. In this case (Fig. 2), each member of the periodic cell rotates about the junctions when is loaded, thereby producing the expansion of the structure in both directions (horizontal and vertical). Thus, one obtains

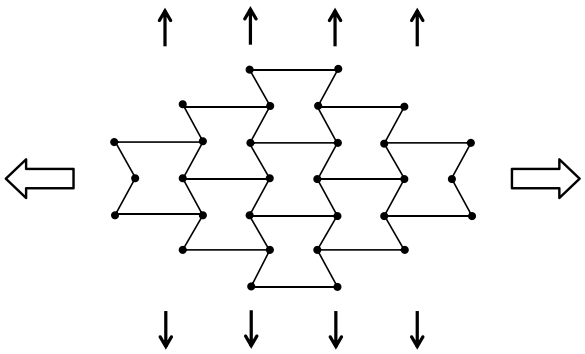

Fig. 2. Auxetic macrostructure obtained by reentrant unit cell.

the auxetic behavior from the mechanism deformation that arises from the geometric configuration of the periodic unit cell, which is played for the entire domain of the macrostructure. Other geometric configurations proposed for reentrant unit cells can be seen in Liu and Hu [14].

The design of the unconventional reentrant structures is traditionally based on the designer experience. However, in order to make the design of these structures more systematic, it has recently been improved by means of the application of optimization methods, such as the TOM. Sigmund [15] used the TOM to design materials with any prescribed properties, such as negative Poisson's ratio, in which the unit cell is modeled as a truss structure. Schwerdtfeger et al. [16] applied the TOM to design a material having a negative Poisson's ratio, using a given auxetic cell structure previously known as the starting point for the optimization process. Kureta and Kanno [17] proposed a method for designing a periodic unit cell of the auxetic macrostructure by solving a topology optimization problem of a structure composed of a large number of interconnected bars (ground structure).

In general, the unit cell structure (microstructure) has the same characteristics of a compliant mechanism, that is, it consists of a monolithic body that delivers a desired motion when is loaded in a certain way. In fact, the mechanism should provide the largest deflection as possible, at a direction and point of interest, and enough stiffness to the entire structure, in order to transfer an input excitation to a desired mechanical output efficiently. Thinking about that, the compliant mechanism concept is absolutely suitable to design of a microstructure that macroscopically works as an auxetic material [18]. Thus, the topology optimization problem of compliant mechanisms can be applied to design more efficient periodic microstructures for a certain specific structural property, such as the auxetic behavior [18–21].

1.3. Avoiding numerical instabilities in topology optimization

As the finite element method (FEM) is usually employed in TOM to discretize the design domain, some numerical instabilities are common in optimal solutions found by this method, such as checkerboard pattern and mesh dependency [4]. Nevertheless, a major instability in the topology optimization applied to compliant mechanisms is concerning to generation of hinges. The hinges are characterized by two elements in the discretized domain connected by a single node (Fig. 3). In TOM, the discretization of the design domain by lower order finite elements is not able to properly model the deformation in the hinges and, therefore, it is misunderstood as a union of two elements rotating together having rigid body motion. According to Yin and Ananthasuresh [22], the material model of the TOM makes the hinges to have a fictitious stiffness, which is very small relative to the other regions of the domain. Thus, the method takes advantage of this to strategically localize the hinges such that higher output displacements are generated to the compliant mechanism.

Some works in the literature have studied that issue by applying alternative filtering schemes and constraints to the topology

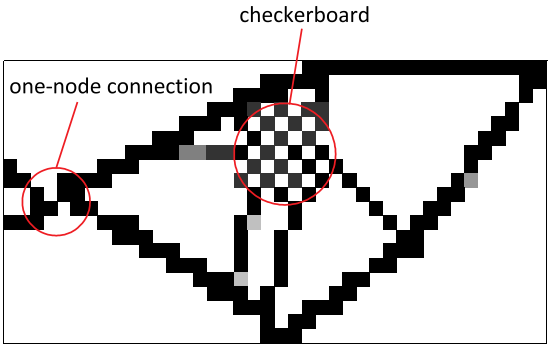

Fig. 3. Numerical instabilities in topology optimization result.

optimization problem [22–25], as well the recent exploiting of the topological sensitivity instead of pseudo-densities [26] to avoid the generation of hinges. In general, mathematical artifices and constraints are employed to design a hinge-free compliant mechanism in topology optimization, which often pose greater difficulties in its numerical implementation.

Kaminakis et al. [20] apply the topology optimization formulation for compliant mechanisms to generate automatically microstructures that lead to auxetic phenomena; however, despite of its interesting design procedure they have not addressed that issue and some hinges are found in their results. Later, Bruggi et al. [21] also investigated the application of topology optimization of compliant mechanisms to synthesize auxetic structures made of micropolar material, in which the Cosserat continuum theory is taken into account; however, using the traditional bi-linear quadrangular elements [27] and conventional density filter [28] that are not able to prevent the arising of hinges. In this present work, the arising of that instabilities (one-node connection) is avoided by exploiting the use of polygonal finite elements [29–31] instead of the traditional FEM framework usually applied in the topology optimization method. Adjacent polygons always keep an edge in common, which directly eliminate the occurrence of hinges.

1.4. Manufacturing of the topology optimization results

Another major challenge is to generate a great topological configuration for the macrostructure whose geometric details are possible to be made by traditional manufacturing techniques. A solution proposed in the literature for improving this characteristic is to include in the topology optimization (TO) problem some manufacturing constraints, which guides the solution of the optimization problem to another solution space generating feasible geometries for the manufacturing point of view. Manufacturing constraints can be done by adding extra constraint equations in the TO problem [32]. However, it increases the complexity of the problem and usually requires high computational cost.

Alternatively, the manufacturing constraint may be implicitly included in the formulation of TO problem by employing the projection technique [33]. This technique was originally developed in order to solve the checkerboard and mesh dependency instabilities [4]. Nevertheless, it has been demonstrating quite effectively to restrict the TO problem in a simple manner for forming regions with desired characteristics, such as minimum thickness and, thus, reducing the geometric complexity of the results found by the TOM.

Vatanabe et al. [34] developed a topology optimization formulation with manufacturing constraints by combining the projection technique and a mapping procedure, which consists in projecting a design variables domain onto a pseudo-densities domain to exclude geometries with undesirable features in the results obtained by the topology optimization algorithm. Thus, the TO problem is guided to obtain solutions with features that can be manufactured by conventional manufacturing processes (extrusion, casting, turning, etc).

Nowadays, the most viable way to manufacture a complex structure, resulting from the TOM, is through the additive manufacturing [35]. In these technique, layers of base material (powder, liquid, or solid) are processed sequentially, using light or heat, to generate the complex structure by stacking and adherence of these layers. The additive manufacturing (AM) has the advantage of providing greater control over the geometry of the object, which is provided to AM equipment in the form of a CAD model, making possible to manufacture very complex geometric shape.

Andreassen et al. [36] built a 3D auxetic structure by using the TOM with a robust design formulation that requires high computational cost, whose manufacturing has been made by Selective Laser Sintering (SLS). Schwerdtfeger et al. [16] used the TOM to improve the design of an existing auxetic structure and have manufactured it by the technique known as Selective Electron Beam Melting (SEBM). Rezaie et al. [37] and Leary et al. [38] proposed interesting methodologies to make the results obtained by the TOM free-supported when printed by the FDM (Fused Deposition Modeling) process; however, sacrificing considerably the original optimal solution obtained through the topology optimization problem.

In fact, there are difficulties to fully enable the solutions obtained by the TOM to be manufactured through the AM because some requirements associated to AM processes, such as minimum wall thicknesses and allowable overhang angles [35]. Thus, the main objective of this work is to create an optimized microstructure that simulate the effect of auxetic material by means of the topology optimization applied to compliant mechanism design, introducing in the optimization problem the polygonal finite element formulation to avoid the hinges (one-node connections), and an integrated approach that combines a projection technique with a mapping technique to include a minimum member size constraint that allows the solution be manufactured by using 3D printers based on FFF (fused filament fabrication) and PolyJet technologies. A pattern repetition constraint is also applied to generate auxetic macrostructures.

The following sections of the paper is organized as follows. Sections 2 and 3 provide a brief theoretical introduction about the polygonal finite elements and the implemented manufacturing constraints, respectively. Section 4 describes the topology optimization problem and its numerical implementation. Section 5 presents some results. Finally, Section 6 gives the concluding remarks and points to future developments.

2. Polygonal finite element mesh

Traditionally, the discretization of the design domain in topology optimization has been carried out by using triangular or quadrilateral finite elements, since the theoretical concepts, basic formulations, and numerical implementation of these elements are well established in the literature [27]. However, that such finite element discretization exhibit one-node connections (see Fig. 3) in topology optimization applied to compliant mechanism design. Thus, the polygonal finite element meshes have been studied over the past decade as alternative to overcome this issue. Adjacent polygons always keep an edge in common having two connected vertices (Fig. 4), and due to the virtue of its geometry can directly eliminate the occurrence of one-node connection (hinges) in topology optimization results.

Saxena and Saxena [29] proposed a honeycomb mesh for domain discretization employed for topology synthesis of compliant mechanisms. In their work, the polygonal element is constructed by splitting a hexagonal cell into two four-node quadrilateral elements. This strategy makes their finite element (FE) analysis easier and straightforward to be performed, since the FE formulation for quadrilateral elements can be taken for the analysis of the hexagonal element; however, different topology optimization results are obtained according the split line direction adopted for the hexagonal cell.

A regular hexagonal cell has more lines of symmetry than triangular

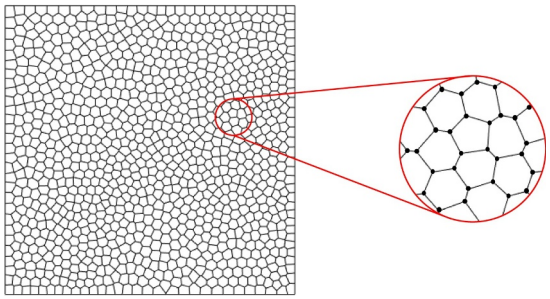

Fig. 4. Edge connection of a polygonal mesh and detail displaying two connected nodes per edge.

and quadrilateral ones, allowing flexible arrangements of the layout in the design domain. Talischi et al. [30] developed a FE formulation for the hexagonal cell, using Wachspress rational interpolation functions. They describe how to construct the shape functions for the hexagonal element domain from the algebraic equations of its edges, and illustrate some results to demonstrate the stability and robustness of their element for topology optimization problems. In all of these works, it is demonstrated that a hexagonal tessellation does not allow any region in the design domain to be artificially stiff, thus the topology results obtained are free from any hinges, as well the checkerboard pattern.

Polygonal elements also have the advantage of overcome the difficulty of the traditional finite elements (triangular or quadrilateral for 2D and tetrahedral or hexahedral for 3D) in discretizing design domains with complex geometries. Moreover, structured meshes constructed with traditional elements with regular geometries (square or triangle) may not be able to accurately compute the design response in many engineering applications of topology optimization.

Thus, in this paper, structured and unstructured meshes using arbitrary polygonal elements are priorized in the topology optimization process for complaint mechanism design. The unstructured mesh is generated from a set of points (seeds) distributed randomically in the desired design domain. The discretization scheme of the domain is based on a centroidal Voronoi tessellation around each seed, achieved by an iterative process called Lloyd's method [39]. The shape functions of the polygonal element are formulated by means of the finite element scheme for convex n-gons proposed by Sukumar and Tabarraei [40]. A complete description of the mesh generation scheme and the proposed polygonal FE element can be found in Talischi et al. [31].

3. Manufacturing constraint for topology optimization

One of the most important requirement associated to additive manufacturing (AM) processes is regarding the minimum wall thicknesses of the part. Here, the unified projection-based approach proposed in Vatanabe et al. [34] is adopted for implementing a minimum member size constraint, in order to generate feature sizes (wall thickness) in topology optimization results compatible to be manufactured by AM process (3D print).

In this approach, projection and mapping techniques are combined for generating manufacturing constraints that is able to control the optimization solution without adding a large computational cost. First, design variables (d) and pseudo-densities (ρ) domains are defined. According to the required manufacturing constraint, a mapping procedure of both domains (d and ρ) is carried out to identify which elements in the pseudo-densities domain are influenced by the design variables domain. Second, a set of variables d_j are calculated and projected onto the domain of pseudo-densities (ρ_i) by the following q-norm [34,41]:

$$\rho_i = \left(\sum_{j \in \Omega_k} d_j^q \right)^{\frac{1}{q}} \quad with \quad q > 0 \tag{1}$$

The differentiable max() operator given by Eq. (1) is employed as projection function to compute the maximum value of a set of variables d_j located in the Ω_k region. Each element in the Ω_k domain influences the sensitivity of the variable (d_j).

To implement the minimum member size constraint in the topology optimization problem, a circular region (Ω_k) with a prescribed radius (R) is defined upon each element of the design variables domain, and projected upon each pseudo-density ρ_i. As a largest value is taken for the design variables (d_j) inside of Ω_k, the feature sizes of resultant topology in the pseudo-densities domain will be larger, when mapping is performed, as illustrated in Fig. 5.

Thus, the minimum member size constraint drives the topology optimization algorithm to search for a solution with a minimum length scale for the structural members, as required by the design. The minimum length scale controlling of structural members is a well-known constraint in the literature [33,41,42]; however, in this works the implementation of this constraint is explored by using the projection function given by Eq. (1), which is differentiable on the whole domain [34] and easy to implement computationally.

Additionally, as can be seen in the results shown ahead, a pattern repetition constraint can be applied to obtain a macrostructure in a straightforward manner, by inducing repetition of patterns that mimics the material microstructure configuration inside the design domain. To implement this constraint in the topology optimization problem, the discretized design domain (Ω) is divided by $n \times m$ sub-domains, where n and m denotes the number of sub-domains in horizontal and vertical directions (2D domains), respectively. This sub-domains (patterns) are repeated inside the design domain regarding the same coordinate systems. All elements of the sub-domain are represented by the design variables d_j, and the sensitivity in relation to each design variable must be multiplied by the number of repeated patterns. Moreover, the design domain must be modeled by a FE structured mesh, in which the number

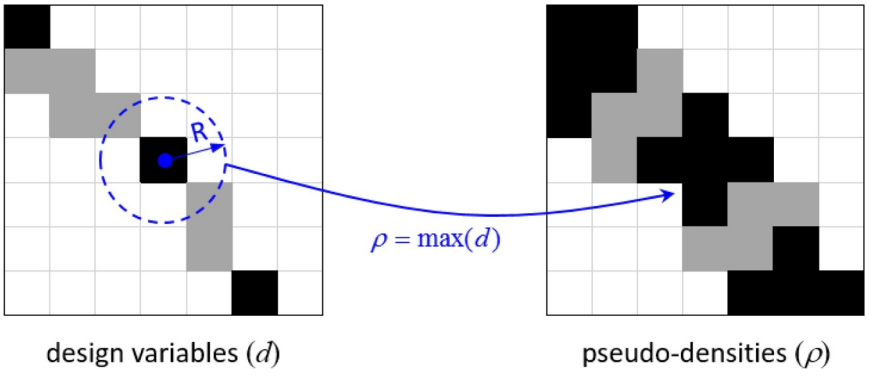

Fig. 5. Mapping and projection scheme for minimum member size constraint.

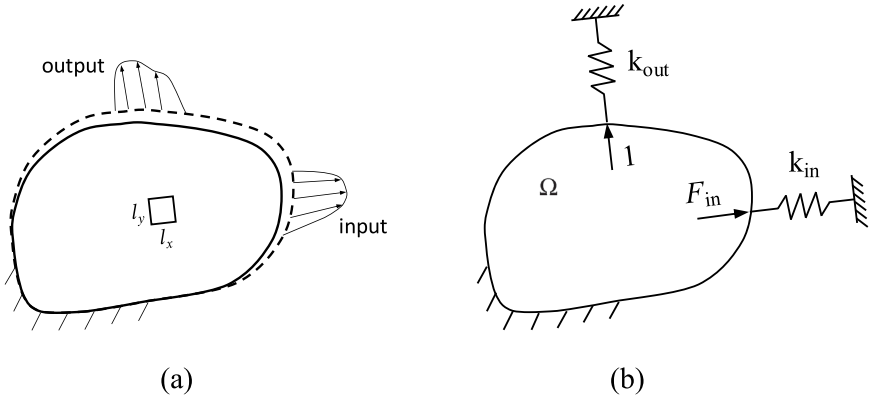

Fig. 6. Auxetic mechanism concept: (a) design domain and boundary conditions; (b) including a spring with stiffness k_{in} to control the input displacement.

of elements must be divided equally by the patterns. More details about the implementation of this manufacturing constraint can be found in Vatanabe et al. [34].

This work contributes by showing in detail how the behavior of topology optimization formulation can be posed to attain well-defined solid-void (0–1) layout in the design domain, by applying the unified projection-based approach found in Vatanabe et al. [34]. The successful implementation of this approach in the topology optimization of compliant mechanism applied to generate microstructures that simulate the effect of auxetic materials is one of main contribution of this paper.

4. Topology optimization problem and its numerical implementation

Let's consider the input and output shown in Fig. 6a to be a tensile load (F_{in}) and a displacement (u_{out}), respectively. Thus, in order to reach the auxetic behavior, when the load F_{in} is applied to the mechanism structure (Ω) it should be necessarily designed to expand (u_{out}) in the perpendicular to the tensile load direction.

For the elastic material subjected to a uniaxial stress, the Poisson's ratio (ν) is defined as the negative ration of the transverse strain (ε_y) over the axial strain (ε_x). Now, considering a very small cartesian region of the structure domain (Fig. 6a) with dimensions l_x and l_y. As the strains ε_x and ε_y are calculated by means of axial (Δ_x) and transversal (Δ_y) elongations, if l_x is equal to l_y the Poisson's ratio can be written as follows [18]:

$$\nu = -\frac{\varepsilon_y}{\varepsilon_x} = -\frac{\Delta_y}{\Delta_x} = -\frac{u_{out}}{u_{in}} \tag{2}$$

where u_{in} is the input displacement produced by the input force (F_{in}).

That is, to reach an optimized structural layout to the compliant mechanism that mimics a microstructure of the auxetic material, the topology optimization problem can be formulated to maximize the Poisson's ratio given by Eq. (2). However, the input displacement u_{in} should be prescribed or limited by the applied load (F_{in}), in order to control the level of stress in the structural mechanism design [6,9]. Thus, this control has been made by introducing a spring with stiffness k_{in}, as shown in Fig. 6b.

Therefore, the objective function of the optimization problem becomes to maximize the output displacement (u_{out}), which is equivalent to maximize the output work carried out in a spring with stiffness k_{out} [4]. To sum up, the topology optimization problem is stated as follows:

$$\begin{aligned}
&\underset{\mathbf{0}\le\mathbf{d}\le\mathbf{1}}{\text{maximize}} u_{out}\\
&\text{subject to} \rho = f(\mathbf{d})\\
&\sum_{i=1}^{N} \rho_i v_i \le f_r V\\
&\text{with} \mathbf{K}(\rho)\mathbf{u} = \mathbf{f}(\textit{equilibrium equations})
\end{aligned} \tag{3}$$

where v_i is the volume of i-th element, V is the volume of the design domain considering all elements as solid phase, f_r is the prescribed volume fraction, and N is the number of elements of the discretized domain. The first constraint, $\rho = f(\mathbf{d})$, is given by Eq. (1). Moreover, in the nested formulation $\mathbf{K}$ is the global stiffness matrix, $\mathbf{u}$ is the global displacement vector, which depends on design variables $\mathbf{d}$, and $\mathbf{f}$ is the global load vector. It is observed that k_{in} and k_{out} are implicitly considered in the equilibrium equations of the problem of Eq. (3).

The second constraint (volume constraint) of the optimization problem, Eq. (3), may help us to control the quantity of material inside the compliant mechanism domain, which allows to obtain different solutions according the design requirement. In this work, it is noticed that topology optimization problem must have enough quantity of material to generate a feasible result. Several formulations have been proposed for the topology optimization of compliant mechanisms [1,6,9,24,43–45]. However, the topology optimization problem of Eq. (3) has simple computational implementation and demonstrated to be efficient to our purpose.

4.1. Sensitivity analysis

Considering the unified based-projection scheme, adopted in this work, the sensitivity of an objective function with respect to the design variables (d_j) is given by Vatanabe et al. [34], that is:

$$\frac{\partial f(\rho(d_j))}{\partial d_j} = \sum_{i\in\Omega} \frac{\partial f}{\partial \rho_i}\frac{\partial \rho_i}{\partial d_j} \tag{4}$$

where Ω is the design domain and $\partial\rho_i/\partial d_j$is the direct differentiation of Eq. (1) [34].

In this work, the sensitivity $\partial f/\partial\rho_i$ is obtained by writing the objective function of the topology optimization problem, as follows:

$$f = u_{out} = -\mathbf{L}^T\mathbf{u} \tag{5}$$

where $\mathbf{L}$ is a vector composed of zeros except for the position at the output (u_{out}) point which is one. Thus, assuming design-independent loads and applying the adjoint method, the sensitivity $\partial f/\partial\rho_i$ is given by:

$$\frac{\partial f}{\partial \rho_i} = -\mathbf{L}^T\frac{\partial \mathbf{u}}{\partial \rho_i} \quad \Rightarrow \quad \frac{\partial f}{\partial \rho_i} = \lambda^T\frac{\partial \mathbf{K}}{\partial \rho_i}\mathbf{u} \tag{6}$$

where the adjoint vector $\boldsymbol{\lambda}$ is the solution of the following adjoint problem $\mathbf{K}\,\boldsymbol{\lambda} = -\mathbf{L}$. The derivative $\partial\mathbf{K}/\partial\rho_i$ is calculated from direct differentiation of the finite element stiffness matrix.

This element stiffness matrix has a penalization imposed by the material model, which makes the relaxation of the original 0–1 (void-solid) problem in topology optimization [4]. In this work, a modified version of the Solid Isotropic Material with Penalization (SIMP) model is adopted, in which a very weak material (Ersatz material) is applied to represent the void region [46,47]. This modified SIMP model defines

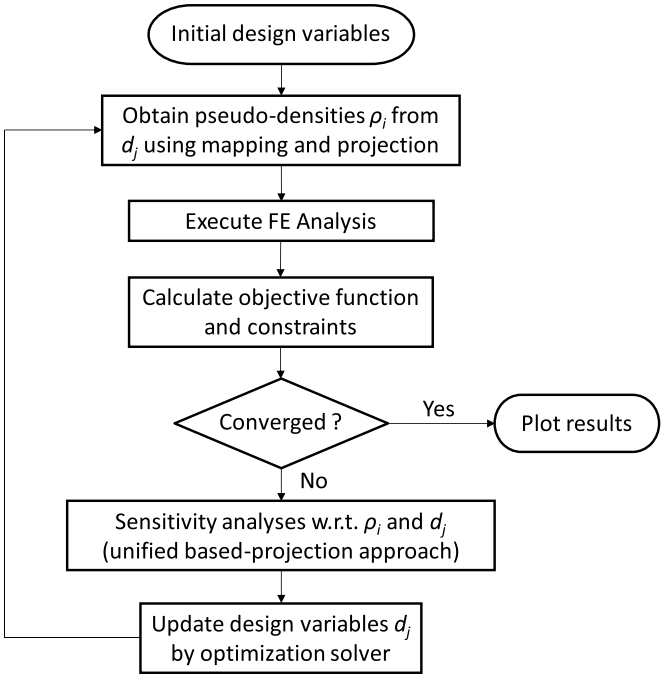

Fig. 7. Flowchart of the topology optimization algorithm.

the material at each element in the discretized domain, as follows:

$$E_i(\rho_i) = E_{\min} + \rho_i^p (E_0 - E_{\min}), \quad \rho_i \in [0, 1], \tag{7}$$

where p is the penalization factor ($p > 1$) between solid and void, E_0 and $E_{\min}$ are the elastic modulus of the solid and void (Ersatz) material, respectively.

4.2. Numerical implementation

The optimization problem, Eq. (3), is solved by an iterative topology optimization (TO) algorithm, implemented in this work using the MATLAB code. Fig. 7 shows the flowchart of this TO algorithm, considering the unified based-projection technique adopted in this work [34]. First, initial (guess) design variables (d_j) are provided as input to TO algorithm, which are used to obtain the initial pseudo-densities (ρ_i) by using the projection function, Eq. (1). The design domain is discretized using polygonal finite elements provided by the Polymesher [48], which is a robust mesh generator solver that uses Centroidal Voronoi diagrams to generate a polygonal mesh.

After that, the implemented TO algorithm follows the usual procedure outlined in the references on topology optimization method. It calculates the objective function value and performs the sensitivity analyses, which are used by the optimization solver as guidance for recalculating material distribution along the design domain. The algorithm generates a new set of design variables after each iteration and the optimization cycle continues until convergence is achieved for the objective function.

The topology optimization procedure (Fig. 7) is adapted in the PolyTop [49], which is an efficient MATLAB code implemented for structural topology optimization. In this work, the method of moving asymptotes (MMA) solver [50] has been employed in the Polytop to update the design variables of the topology optimization problem. Nevertheless, other optimization solvers can be explored for this purpose, such as the well-known optimality criteria (OC) method [4]. It is noticed that after few changes in the move limit and damping parameters of original OC optimizer implemented in the PolyTop, no convergence problems have found during the optimization process for compliant mechanism design. Moreover, positive values in the sensitivity analyses should be replaced by small positive values for the OC solver works correctly [4].

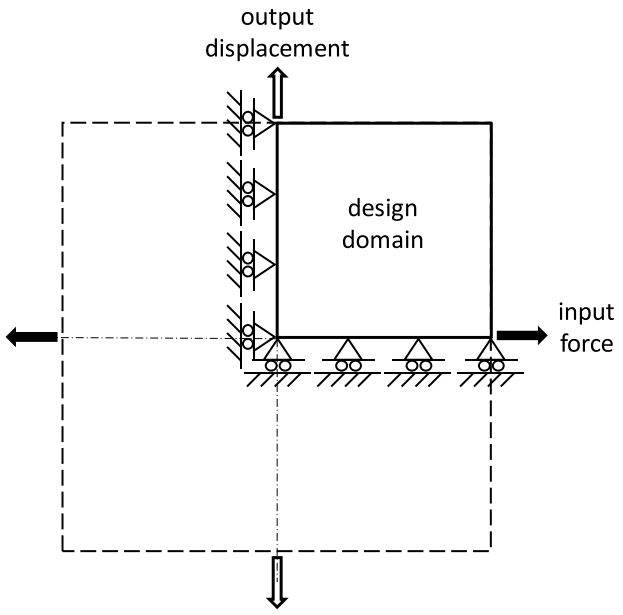

Fig. 8. Design domain and boundary conditions considered for topology optimization process.

5. Results

Fig. 8 shows the design domain for the compliant mechanism design that simulates an auxetic microstructure. Due to symmetry and to save computational time, only a quarter of the entire structure (square domain) is used for obtaining the topology optimization solution. The position of the input force and the desired displacement (output) as well as fixed supports configuration to impose the symmetry condition are also shown in the Fig. 8.

The input force and the output displacement are perpendicular to each other, and occur toward the directions indicated in the Fig. 8, allowing the calculation of the Poisson's ration as defined previously (Section 4). That is, the desired structure to the compliant mechanism should expand in the direction indicated for the output displacement when the input force is applied at the orthogonal direction shown in the Fig. 8.

In the all examples shown ahead, the value of the input force (F_{in}) is equal to 1. Consistent units are employed. The elastic modulus of the Ersatz material is $E_{\min} = 10^{-4} E_0$, and the Poisson's ration of the solid material in the topology optimization is equal to 0.3. Moreover, a penalty factor $p = 3$ is adopted for the SIMP model.

Linear finite element (FE) analysis, in plane strain, are carried out to reach our goal. Eventhough, linear FE analysis may not be as accurate as a non-linear analysis to simulate the response of the structure, since compliant mechanisms often undergo large deformations, the linear analysis is enough to demonstrates the presence of auxetic behavior in the topology optimization results presented in this work. Kaminakis and Stavroulakis [18] also conclude the same.

5.1. Unit auxetic cell design

In this example, the design domain is discretized in 3000 polygonal elements, as shown in Fig. 9. The Voronoi polygonal mesh is generated through a random placement of seeds in the PolyMesher algorithm [48], which allows obtaining a non-structured mesh with different polygonal elements. In this case, most of them are hexagonal (1,881 elements); however, pentagons (690 elements), heptagons (399 elements), tetragons (28 elements) and octagons (2 elements) can be found in this polygonal mesh (Fig. 9). The bottom and left sides of the polygonal mesh are constrained along the vertical and horizontal directions,

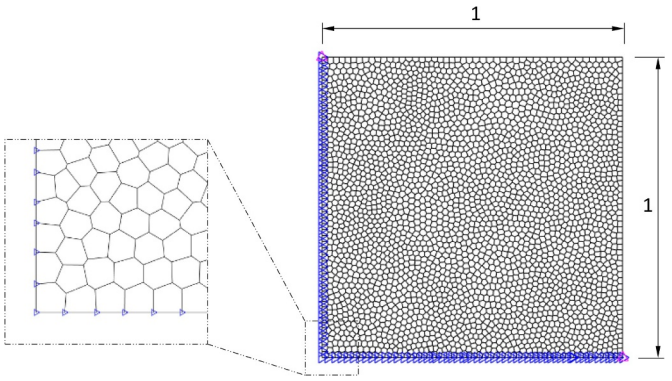

Fig. 9. Polygonal FE mesh (1881 hexagons, 690 pentagons, 399 heptagons, 28 tetragons and 2 octagons).

respectively, as indicated in Fig. 9.

Springs with stiffness $k_{in} = 0.1$ and $k_{out} = 0.1$ are considered at the input force and output displacement regions. A volume fraction (f_r) equal to 30% of the fully solid domain volume is applied. Fig. 10 shows the result obtained by considering radius (R) equal to 0.03 to the minimum member size constraint and random values to the design variables at the start (initial guess) of the topology optimization algorithm. In this work, uniformly distributed random values are applied as initial guess, since it makes the implemented optimization algorithm efficient to find representative local minima (larger negative Poisson ratio), such as the local optimum shown of Fig. 10.

Fig. 10a and b show the relation between design variables *d* and the final solution obtained for the pseudo-densities (ρ). This result gives an idea how the implemented based-projection approach can lead to solutions with a minimum length scale for the structural members (Fig. 10c), which is easier to be manufactured by an AM process, such as 3D print. Moreover, due to the mapping and projection schemes successfully adapted for this work, the implemented TOM algorithm generates optimized topologies having better black and white design. Besides, the result shown in Fig 10b can be post-processed to illustrate a better image (Fig. 10c), from the point of engineering view, of the topology optimization result. This post-processing is carried out after the last iteration of the optimization process, by applying a cutoff value (threshold) for the pseudo-densities. For all the examples presented in this work, high cutoff value (0.99) has been applied, which means that only pseudo-density values close to 1 are considered in the post-processed final result.

As can be seen in Fig. 10b, this result is also free for checkerboard pattern. It is noticed that polygonal element has a checkerboard-free property, which is attributed essentially to its geometric features and interpolation characteristics [31]. It is also verified that the microstructure obtained from topology optimization of compliant mechanism, shown in Fig. 10, has auxetic behavior with Poison's ratio of $\nu = -0.150$. This value is calculated by applying Eq. (3), considering the heterogeneous domain (Fig. 10b) resulting from the topology optimization process.

If necessary, the design of this auxetic microstructure can be improved by controlling the work carried out by the output force on the compliant mechanism. The output work can be controlled by the stiffness value of the spring at the output region (k_{out}). Fig. 11 shows the result obtained by reducing the output spring stiffness to the half ($k_{out} = 0.05$) and keeping $k_{in} = 0.1$. In this example, larger Poison's ration ($\nu = -0.242$) has been achieved to the auxetic microstructure (Fig. 11b). It is also demonstrated from additional simulations, in which smaller and larger values are adopted to the spring stiffness k_{in} and k_{out}. That is, as k_{in} and k_{out} values are changed the behavior of the optimized auxetic structure (negative Poisson's ratio values) can be affected considerably, mainly when small k_{out} values are applied.

Moreover, by using polygonal elements, naturally one-node connections do not occur, as can also noticed in these optimized results (Figs. 10 and 11). Nevertheless, topology optimization of a compliant mechanism undergoes formation of region having only one element at the thickness, as shown in the detail of Fig. 11b, which increases considerably the output displacement (u_{out}). However, this thinner region makes the mechanism less resistant to fatigue damage and more difficult to be manufactured. To overcome this issue, the radius (R) of the minimum member size constraint implemented in this work can be slightly increased, to find an improved solution without excessive compromising the previous result. Fig. 12 shows the results obtained by using R = 0.035.

Two different examples are evaluated in this case. In the first example (Fig. 12a), the topology optimization process of compliant mechanism is carried out considering $k_{in} = k_{out} = 0.1$, which provides a solution with Poison's ration of $\nu = -0.124$. In the second one (Fig. 12b), an alternative solution has been found using $k_{out} = 0.05$ (keeping $k_{in} = 0.1$), providing an auxetic microstructure with larger Poison's ration of $\nu = -0.211$. In this example (Fig. 12b), the output displacement has been increased in order to improve the auxetic behavior of the structure. Thus, a thinner member arises on the top of optimized structure to make this part of structure more flexible. In other hand, as the volume fraction is kept the same ($f_r = 30\%$) applied to obtain the optimized structure shown Fig. 12a, an unnecessary quantity of material (bump) is appended on the thinner member. This bump might be excluded of the final result through a post-processing after the last iteration of the topology optimization process. Alternatively, it can be also avoided during the optimization process by reducing slightly the volume fraction (f_r) allowed to the optimized auxetic

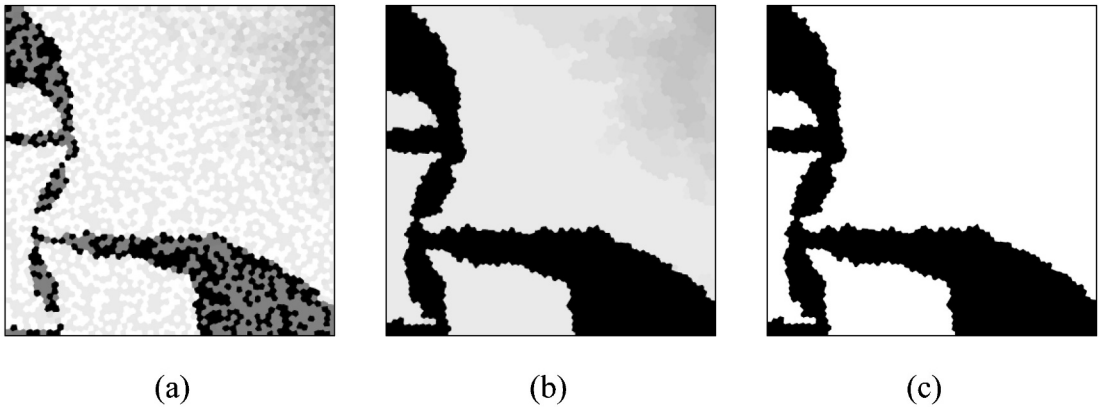

Fig. 10. Results obtained by using $f_r = 30\%$ volume constraint to the domain discretized into 3000 elements: a) design variable *d*; b) pseudo-density ρ; c) post-processed view of the pseudo-densities.

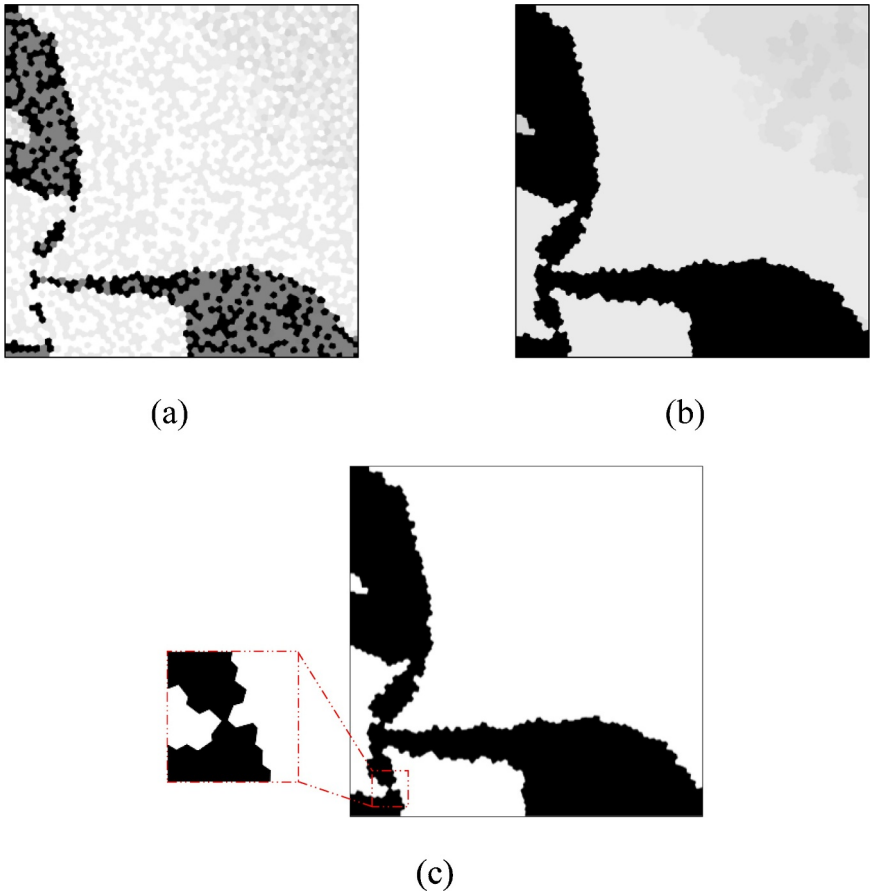

Fig. 11. Results obtained by using $k_{out} = 0.05$ ($k_{in} = 0.1$), $f_r = 30\%$ volume constraint to the domain discretized into 3000 elements: a) design variable d; b) pseudo-density ρ; c) post-processed view of the pseudo-densities and thin thickness detail.

structure.

Fig. 13a shows a view of the entire auxetic microstructure domain obtained from the result presented in Fig 12b. A post-processed view is performed in a CAD software to produce a well-defined contour for the topology optimization result (Fig. 12b) and to generate a geometric model to be verified by FE analysis. Fig. 13b shows the underformed and deformed shapes of the auxetic microstructure designed by topology optimization of compliant mechanism. The post-processing is carried out after the last iteration of the optimization process and the deformed shape is obtained by computational simulation through a commercial FE software (ANSYS).

5.2. Results with pattern repetition constraint

The unit cell of the microstructure shown in Fig. 13a, designed by topology optimization, can be repeated several times into a domain to generate a macrostructure that simulates an auxetic material. Nevertheless, another alternative has been explored to the same purpose, in

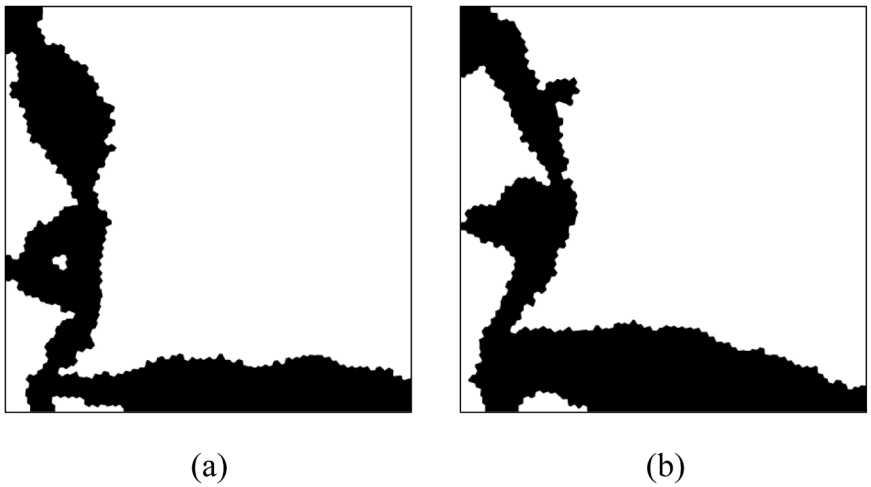

Fig. 12. Results obtained by using R = 0.035, $f_r = 30\%$ volume constraint to the domain discretized into 3000 elements: (a) $k_{in} = k_{out} = 0.1$; (b) $k_{in} = 0.1$ and $k_{out} = 0.05$.

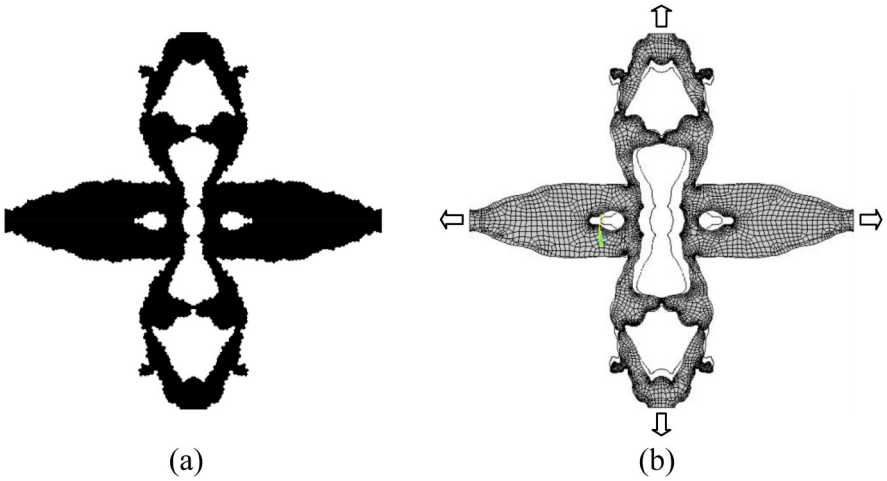

Fig. 13. Auxetic microstructure design: (a) complete view of the auxetic structure domain; (b) deformed shape obtained through FE analysis.

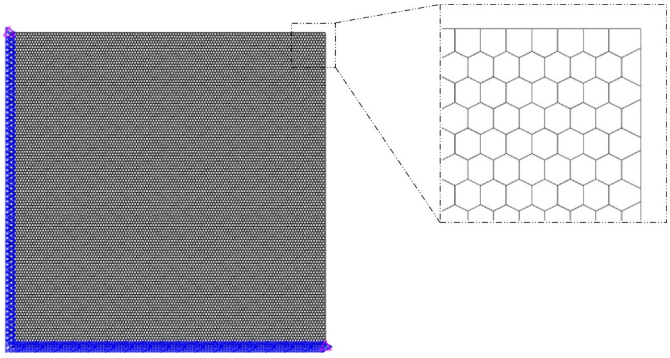

Fig. 14. Structured polygonal FE mesh (14,042 hexagons, 238 pentagons and 120 tetragons).

which a pattern repetition constraint is included in the topology optimization process. Domains with repeated cells can be produced by pattern repetition constraint in a controlled manner, in such way that different regions subjected to different load conditions should assume the same topology for all situations. In this case, a structured mesh is recommended to drive equally all patterns inside a “continuous” domain.

Here, the structured polygonal mesh with 120 × 120 elements is also applied to discretize the design domain shown in Fig. 8. All elements in this mesh (Fig. 14) are hexagons, except the elements at the contour of the domain, in which pentagons and tetragons are also applied to obtain well-defined shape to the contour.

The boundary conditions (supporting and loading) are also shown in Fig. 14. Analogous to the previous examples (Section 5.1), a square domain with the same dimensions and symmetry conditions are taken into account. Thus, bottom and left sides of the mesh are constrained along the vertical and horizontal directions, respectively. Springs with stiffness equal to 0.05 (k_{in} and k_{out}) are applied at the input load and output displacement regions of the domain. Volume fraction (f_r) is 50% and distribution of homogeneous material ($d_{j0} = 0.5$) is adopted at the start (initial guess) of the topology optimization process. Fig. 15 shows the result obtained by using pattern repetition constraint (2 × 2 patterns), considering R = 0.01 to the minimum member size constraint.

In this result (Fig 15a), it is noticed a more uniform mass distribution in the design domain, by comparison with the unit cell of previous results (Section 5.1). Here, the volume constraint has been increased, since more than one cell and small relevance regions into the domain need to be filled with mass. Fig. 15b shows the underformed and deformed shapes of the auxetic structure resulting from topology optimization of compliant mechanism with pattern repetition. The macrostructure obtained (Fig. 15) has auxetic behavior with Poison's ratio of $\nu = -0.165$, which can be improved by controlling the work performed by the output force on the compliant mechanism, as previously demonstrated in the Section 5.1.

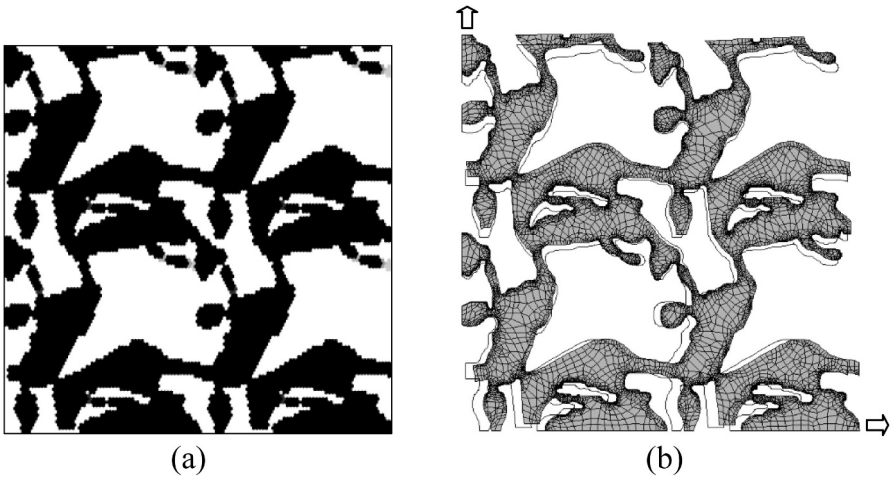

Fig. 15. Results obtained by using 2 × 2 patterns and considering the entire domain discretized into 14,400 elements; b) deformed shape obtained through FE analysis.

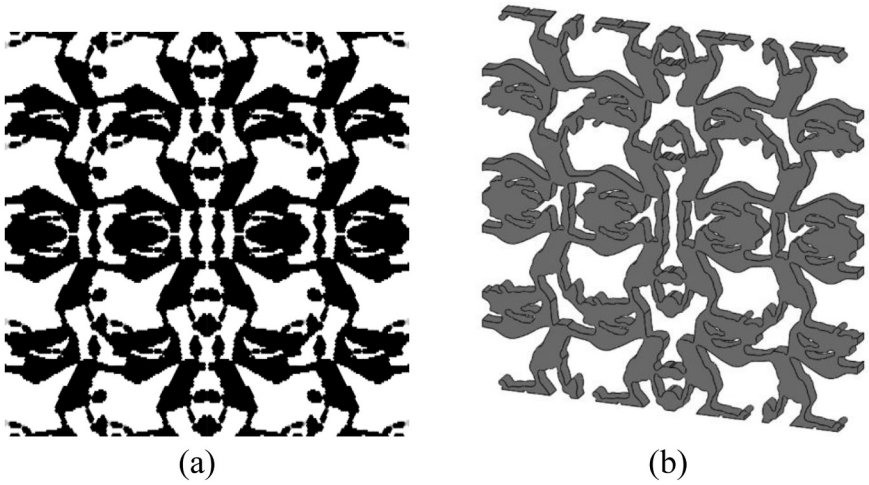

Fig. 16. Auxetic macrostructure design: (a) complete view of the auxetic structure domain; (b) perspective view of the geometric model generated in a CAD software.

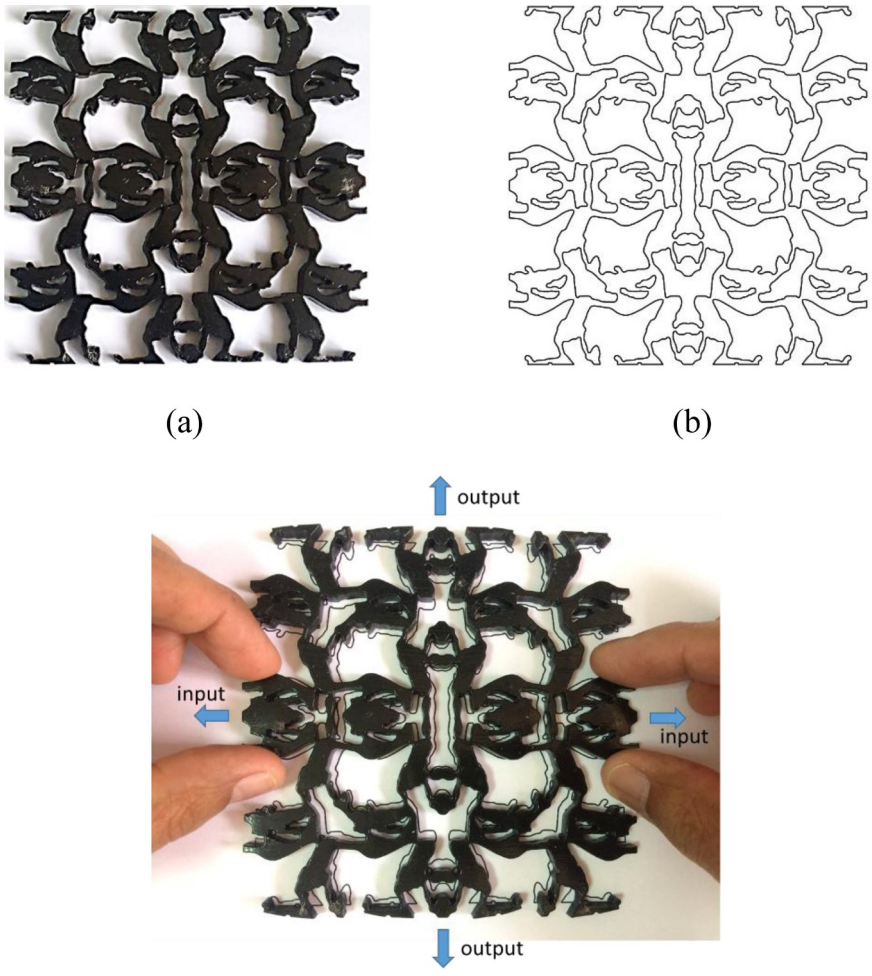

Fig. 17. Auxetic structure verification: (a) prototype manufactured by a 3D printer; (b) undeformed shape view; (c) overlapping undeformed and deformed shape to show the prototype expanding in the orthogonal directions (output) under tensile load (input).

Fig. 16 shows a view of the entire structure domain obtained from the result presented in Fig 15a. A post-processed view is carried out using a CAD software to generate the geometric model shown in Fig. 16b. Based on the FE analysis, illustrated in Fig. 15b, some small regions (material) with no relevant structural function are suppressed during the post-processing phase (solid modeling in a CAD software). This also allows to save cost during a manufacturing prototyping phase.

Thus, manufacturing prototype of the post-processed result

(Fig. 16b) is also carried out to verify experimentally the behavior of the auxetic structure. The prototype has 114 × 114 × 5 mm (height x width x depth) and it is made with TangoBlackPlus material (Fig. 17a), by using a 3D Printer (Polyjet Technology / Stratasys). The TangoBlackPlus is a flexible material (rubber-like resin), which allows large deformation (in linear elastic region) even the structure undergoes small loading. Thus, it makes easy to verify the auxetic behavior of the structure, as shown in Fig. 17. Obviously, it can be carried out using other printable soft and hard materials (NinjaFlex (thermoplastic polyurethane material), ABS (acrylonitrile butadiene styrene), PLA (polylactide), metal, etc); however, a sophisticated apparatus for testing the prototype may be applied.

As illustrated in Fig. 17c, the structural layout obtained by topology optimization of compliant mechanism has been verified, which it expands transversely when subjected to longitudinal elongation. In other words, considering the center of prototype geometry as origin of a coordinate system, only positive displacements are produced in the prototype under tensile load, making the Poisson's ratio negative (auxetic behavior). The input and output displacements u_{in} and u_{out}, used in Eq. (2) to calculate the Poisson's ratio, are predicted through the FE analysis step of the TO algorithm. That is, all densities values ($0 \leq \rho_i \leq 1$) of the material distribution (void-solid) found in the topology optimization results, presented in this work, are included in the calculation of the negative Poisson's ratio of the auxetic heterogeneous structure. Finally, the verification of the effective Poisson's ratio of the results obtained by topology optimization has been done by Kaminakis et al. [20], using classical numerical homogenization.

6. Conclusions

Topology optimization of compliant mechanism has been applied to design micro and macrostructure that simulate the behavior of auxetic materials (negative Poisson's ration). Polygonal finite elements are employed, improving the solution of optimization process, to avoid the formation of the so-called one-node connections in the compliant mechanism design, as well as the checkerboard problem. An efficient MATLAB code, based on the framework of the Polytop, is implemented to handle compliant mechanism design in order to create auxetic structures. Minimum member size constraint has been included in the topology optimization problem by combining projection and mapping techniques. According to the results presented here, this constraint shows to be effective to find better manufacturable solutions, with no excessive sacrifice of the performance (auxetic behavior) of the structure. Pattern repetition constraint is also employed to generate in a straightforward manner a macrostructure that presents negative Poisson's ration. The auxetic behavior of the obtained topology optimization results has been verified through computational simulations using commercial FE software and prototype manufactured by 3D printer (additive manufacturing).

This work provides results that are focused on bidimensional compliant mechanisms under the linear elasticity assumption due to the convenience of simple numerical implementation and efficiency to demonstrate quickly the functionality of the proposed approach. Thus, a natural and important extension for this work is to implement tridimensional (3D) models, by exploring Mimetic Finite Difference (MFD) methods [51] to implement polyhedral shape functions efficiently, and massively parallel computer architectures on GPUs to accelerate the computational processing of the topology optimization algorithm. The main challenge is to apply large scale topology optimization of compliant mechanism for 3D auxetic structure design that can be handle computationally at a low cost. Moreover, non-liner finite elasticity may be considered to topology optimization with polygonal finite element formulation, in order to obtain more accurate models to the structural response of compliant mechanisms under large deformation. Finally, the availability of additive manufacturing techniques that are able of producing parts with more than one material makes room for extending this work to multi-material compliant mechanism design. By allocating optimal material properties to each member of compliant mechanisms, the performance of the optimized auxetic structure may be improved.

Acknowledgments

The first author thanks the São Paulo Research Foundation (FAPESP) for the financial support provided by research grant 2015/08316-2. The authors also thank Krister Svanberg from KTH Royal Institute of Technology for supplying the MMA-code.

References

[1] Howell LL. Compliant mechanisms. New York: John Wiley & Sons; 2001.
[2] Gad-el-Hak M. The MEMS handbook. New York: CRC Press; 2002.
[3] Haftka RT, Gürdal Z, Kamat MP. Elements of structural optimization. Dordrecht: Kluwer Academic; 1992.
[4] Bendsøe MP, Sigmund O. Topology optimization: theory methods and applications. Berlin: Springer-Verlag; 2003.
[5] Ananthasuresh GK. A new design paradigm for micro-electromechanical systems and investigations on the compliant mechanisms PhD. Thesis University of Michigan; 1994.
[6] Sigmund O. On the design of compliant mechanisms using topology optimization. Mech Struct Mach 1997;25(4):493–524.
[7] Frecker M, Kikuchi N, Kota S. Topology optimization of compliant mechanisms with multiple outputs. Struct Multidiscip Optim 1999;17(4):269–78.
[8] Jonsmann J, Sigmund O, Bouwstra S. Compliant thermal microactuators. Sens Actuators 1999;76:463–9.
[9] Pedersen CBW, Buhl T, Sigmund O. Topology synthesis of large-displacement compliant mechanisms. Int J Numer Methods Eng 2001;50(12):2683–705.
[10] Mir M, Ali MN, Sami J, Ansari U. Review of mechanics and applications of auxetic structures. Adv Mat Sci and Eng 2014:1–17.
[11] Evans KE, Alderson A. Auxetic materials: functional materials and structures from lateral thinking!. Adv Mater 2000;12(9):617–28.
[12] Chan N, Evans K. Microscopic examination of the microstructure and deformation of conventional and auxetic foams. J Mater Sci 1997;32(21):5725–36.
[13] Alderson KL, Alderson A, Smart G, Simkins VR, Davies PJ. Auxetic polypropylene fibres: Part 1 – Manufacture and characterization. Plast Rubber Compos 2002;31(8):344–9.
[14] Liu Y, Hu H. A review on auxetic structures and polymeric materials. Sci Res Essays 2010;5(10):1052–63.
[15] Sigmund O. Materials with prescribed constitutive parameters: an inverse homogenization problem. Int J Solids Struct 1994;31(17):2313–29.
[16] Schwerdtfeger, et al. Design of auxetic structures via mathematical optimization. Adv Mater 2011;23:2650–4.
[17] Kureta R, Kanno Y. A mixed integer programming approach to designing periodic frame structures with negative Poisson's ratio. Optim Eng 2014;15:773–800.
[18] Kaminakis NT, Stavroulakis GE. Topology optimization for compliant mechanisms, using evolutionary-hybrid algorithms and application to the design of auxetic materials. Compos Part B 2012;43:2655–68.
[19] Larsen UD, Sigmund O, Bouwstra A. Design and fabrication of compliant mechanisms and material structures with negative Poisson's ratio. J Microelectromech Syst 1997;6(2):99–106.
[20] Kaminakis NT, Drosopoulos GA, Stavroulakis GE. Design and verification of auxetic microstructures using topology optimization and homogenization. Arch Appl Mech 2015;85:1289–306.
[21] Bruggi M, Zega V, Corigliano A. Synthesis of auxetic structures using optimization of compliant mechanisms and a micropolar material model. Struct Multidisc Optim 2017;55:1–12.
[22] Yin L, Ananthasuresh GK. Design of distributed compliant mechanisms. Mech Based Des Struct Mach 2003;31(2):151–79.
[23] Poulsen TA. A simple scheme to prevent checkerboard patterns and one-node connected hinges in topology optimization. Struct Multidisc Optim 2002;24:396–9.
[24] Luo Z, Chen L, Yang J, Zhang Y, Abdel-Malek K. Compliant mechanism design using multi-objective topology optimization scheme of continuum structures. Struct Multidisc Optim 2005;30:142–54.
[25] Sigmund O. Morphology-based black and white filters for topology optimization. Struct Multidiscip Optim 2007;33(4):401–24.
[26] Krishnakumar A, Suresh K. Hinge-free compliant mechanism design via the topological level-set. J Mech Des 2015;031406:1–10. 137.
[27] Bathe KJ. Finite element procedures. New Jersey: Prentice Hall; 1996.
[28] Bourdin B. Filters in topology optimization. Int J Numer Methods Eng 2001;50(9):2143–58.
[29] Saxena R, Saxena A. On honeycomb representation and SIGMOID material assignment in optimal topology synthesis of compliant mechanisms. Finite Elem Anal Des 2007;43:1082–98.
[30] Talischi C, Paulino GH, Le CH. Honeycomb Wachspress finite elements for structural topology optimization. Struct Multidisc Optim 2009;37:569–83.
[31] Talischi C, Paulino GH, Pereira A, Menezes IFM. Polygonal finite elements for topology optimization: a unifying paradigm. Int J Numer Methods Eng 2010;82:671–98.
[32] Zuo K-T, Chen L-P, Zhang Y-Q, Yang J. Manufacturing- and machining-based

topology optimization. Int J Adv Manuf Technol 2006;27(5-6):531–6.
[33] Guest JK, Prevost JH, Belytschko T. Achieving minimum length scale in topology optimization using nodal design variables and projection functions. Int J Numer Methods Eng 2004;61(2):238–54.
[34] Vatanabe SL, Lippi TN, Lima CR, Paulino GH, Silva ECN. Topology optimization with manufacturing constraints: a unified projection-based approach. Adv Eng Softw 2016;100:97–112.
[35] Brackett D, Ashcroft I, Hague R. Topology optimization for additive manufacturing. Proceedings of the 22nd annual international solid freeform fabrication symposium - an additive manufacturing conference. 2011. p. 348–62.
[36] Andreassen E, Lazarov BS, Sigmund O. Design of manufacturable 3D extremal elastic microstructure. Mech Mater 2014;69:1–10.
[37] Rezaie R, Badrossamay M, Ghaie A, Moosavi H. Topology optimization for fused deposition modeling process. Procedia CIRP 2013;6:521–6.
[38] Leary M, Merli L, Torti F, Mazur M, Brandt M. Optimal topology for additive manufacture: a method for enabling additive manufacture of support-free optimal structures. Mater Des 2014;63:678–90.
[39] Lloyd S. Least squares quantization in PCM. IEEE Trans Inf Theory 1982;28(2):129–37.
[40] Sukumar N, Tabarraei A. Conforming polygonal finite elements. Int J Numer Methods Eng 2004;61(12):2045–66.
[41] Le CH. Achieving minimum scale and design constraints in topology optimization: a new approach. University of Illinois at Urbana-Champaign (UIUC); 2006. MS Thesis.
[42] Zhou M, Shyy Y, Thomas H. Checkerboard and minimum member size control in topology optimization. Struct Multidisc Optim 2001;21(2):152–8.
[43] Frecker MI, Ananthasuresh GK, Nishiwaki S, et al. Topological synthesis of compliant mechanisms using multi-criteria optimization. J Mech Des 1997;119(2):238–45.
[44] Nishiwaki S, Frecker MI, Min S, Kikuchi N. Topology optimization of compliant mechanisms using the homogenization method. Int J Numer Methods Eng 1998;42:535–59.
[45] Min S, Kim Y. Topology optimization of compliant mechanism with geometrical advantage. JSME Int J Series C 2004;47(2):610–5.
[46] Bendsøe MP. Optimal shape design as a material distribution problem. Struct. Optim 1989;1:193–202.
[47] Zhou M, Rozvany GIN. The COC algorithm, part II: topological, geometry and generalized shape optimization. Comput Meth Appl Mech Eng 1991;89(1):197–224.
[48] Talischi C, Paulino GH, Pereira A, Menezes IFM. PolyMesher: a general-purpose mesh generator for polygonal elements written in Matlab. Struct Multidisc Optim 2012;45:309–28.
[49] Talischi C, Paulino GH, Pereira A, Menezes IFM. PolyTop: a Matlab implementation of a general topology optimization framework using unstructured polygonal finite element meshes. Struct Multidisc Optim 2012;45:329–57.
[50] Svanberg K. The method of moving asymptotes - a new method for structural optimization. Int J Numer Methods Eng 1987;24:359–73.
[51] Gain AL, Paulino GH, Duarte LS, Menezes IFM. Topology optimization using polytopes. Comput Methods Appl Mech Eng 2015;293:411–30.